Andrzej POPENDA

Czestochowa University of Technology

Modelling of BLDC motor energized by different converter systems

Abstract. In the paper a BLDC motor, energized by different converter systems, is studied. These converter systems are based on: PWM-controlled three-phase inverter, PWM-controlled DC/DC converter and PWM-controlled DC/DC converter with low-pass filter LC, respectively. Mathematical models of the respective structures are formulated and the results of computer simulation, partially verified by experimental test and other simulation, are presented and discussed.

*Streszczenie. W pracy rozważono silnik BLDC zasilany przez różne systemy przekształtnikowe oparte na: trójfazowym falowniku napięcia sterowanym metodą PWM, przekształtniku DC/DC sterowanym metodą PWM bez filtru wyjściowego oraz z zastosowaniem dolnoprzepustowego filtru LC na wyjściu. Sformułowano modele matematyczne poszczególnych struktur jak również zaprezentowano wyniki i dyskusję symulacji komputerowej, częściowo zweryfikowanej eksperymentalnie oraz za pomocą innej symulacji. (**Modelowanie silnika BLDC zasilanego przez różne układy przekształtnikowe**).*

Keywords: BLDC motor, converter and inverter, mathematical modelling, control strategies.
Słowa kluczowe: silnik BLDC, przekształtnik, modelowanie matematyczne, strategie sterowania.

Introduction

Computer simulation is a research method, which can effectively shorten analysis and development cycle of converter-fed drive systems as well as evaluate rationality of control algorithm without causing damage to the motor or controller under test. This method provides a good base for system design and verification of a novel control strategy. In addition, the computer simulation may also be used for educational purposes at minimum cost. The formulation of a mathematical model and then a computer model, using the chosen computer simulation tool, is the starting point to the simulation investigations.

Brushless direct current (BLDC) motors, being a type of permanent magnet synchronous motor [1-6], are commonly used in industry. The examples of industry branches for usage of BLDC motors are appliances, automotive, aerospace, consumer and medical industry as well as industrial automation equipment and instrumentation. Most BLDC motors include three-phase stator winding connected in star fashion. Each phase winding is constructed with numerous interconnected coils placed in the slots of stator. There are two types of motors: trapezoidal and sinusoidal [1,2]. The difference comes from both the interconnection of coils in stator phase windings and the option of magnets magnetization or the shape of rotor magnet pole shoes giving the different types of back electromotive force (EMF), in trapezoidal or sinusoidal fashion, respectively. The analogical classification is applied to the control of electronic commutation circuit. The back EMFs and phase currents of sinusoidal motor are sinusoidal, thus the output torque is smooth in contrast to the deformed back EMFs and phase currents as well as the rippled torque of trapezoidal motor, causing the additional vibrations and noise.

The stator phase windings should be energized in a proper sequence in order to rotate the BLDC motor. The rotor position angle is required to determine a pair of phase windings, which have to be energized according to the abovementioned sequence. Three Hall effect sensors (HES), embedded into the stator on the non-driving end of motor, are widely used to determine the rotor position angle of BLDC motor (HES control) [1,2,7-9]. In addition to the HES control, the pulse width modulation (PWM) is widely used in order to limit the starting current as well as to control speed and torque of BLDC motor. In the paper three types of converter systems energizing the BLDC motor are studied. These converter system are based on: PWM-controlled three-phase inverter, PWM-controlled DC/DC converter and PWM-controlled DC/DC converter with low-pass filter LC, respectively. Mathematical models of the respective structures are formulated and the results of computer simulation, partially verified by experimental test and other simulation, are presented and discussed.

Mathematical models of BLDC motor unit, including stator winding and electronic commutation circuit

The power electronic switches, consisting of transistors and diodes, are used in order to commutate the current in phase windings of BLDC motor. These switches are usually connected in a three-phase bridge for a three-phase BLDC motor shown in Fig. 1. The high-side switches are often controlled using pulse width modulation in order to convert a DC voltage into voltage pulses with variable width.
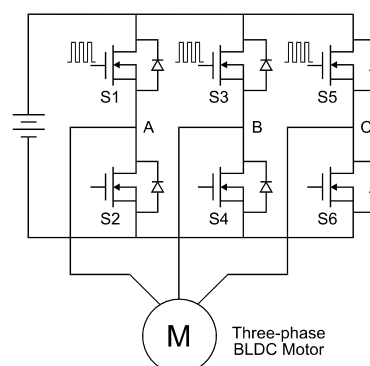

Fig. 1. Three-phase BLDC motor energized by the PWM-controlled inverter bridge

The equivalent circuit of BLDC motor unit, based on the real system (Fig. 1), is depicted in Fig. 2a, where the power electronic switches are replaced by the electric switches shunted with the resistance R_{off} of turn-off transistor. However, the other equivalent circuit of the considered system may be taken into account (Fig. 2b). The parameter R_0 represents the resistance of neutral conductor, if exists. In the system without neutral conductor, this resistance is infinite ($R_0 = \infty$). In practice, a sufficiently high value ($R_0 \gg U_{(ph)n}/I_n$) may be adopted.

The block diagram of BLDC motor control corresponding to the system based on PWM-controlled three-phase inverter (Fig. 1) is depicted in Fig. 3, whereas the other solutions of BLDC motor control are shown as block diagrams in Figs. 4 and 5. Fig. 6 shows block diagram of pulse width modulator to control three-phase inverter bridge or DC/DC converter.
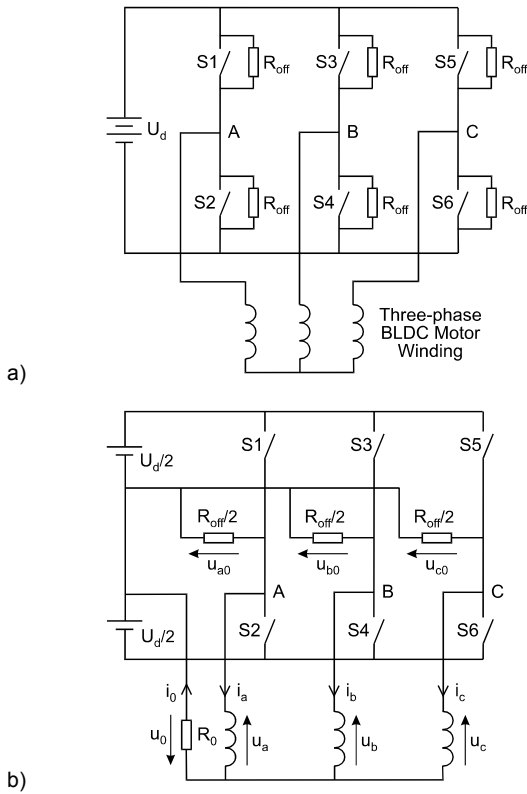
a)

b)

Fig. 2. Equivalent circuits of BLDC motor unit including stator winding and electronic commutation circuit based on three-phase inverter bridge
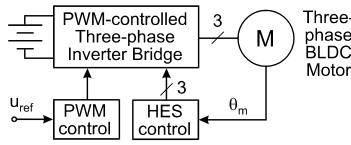

Fig. 3. Block diagram of BLDC motor control based on PWM-controlled three-phase inverter
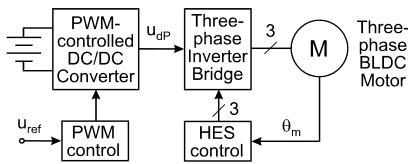

Fig. 4. Block diagram of BLDC motor control based on PWM-controlled DC/DC converter
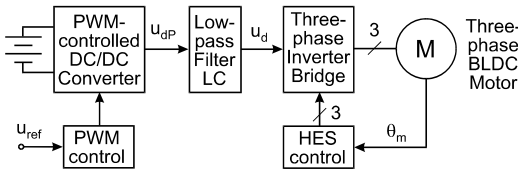

Fig. 5. Block diagram of BLDC motor control based on PWM-controlled DC/DC converter and low-pass filter LC
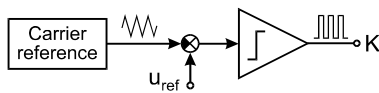

Fig. 6. Block diagram of pulse width modulator to control DC/AC inverter or DC/DC converter

The first considered control strategy (Fig. 3) in the first sequence period:

(a) S1 = S4 = on, S2 = S3 = S5 = S6 = off (HES code: 100) may be described by the following dependencies:

(1)
$$\text{if}(30° < \theta_e \leq 90°)\{u_0 = R_0(i_a + i_b + i_c); \; u_b = \tfrac{-U_d}{2} - u_0;$$
$$u_{a0} = \tfrac{R_{off}}{2}i_a; \text{if}(u_{a0} > \tfrac{U_d}{2}) \; u_{a0} = \tfrac{U_d}{2}; \text{if}(u_{a0} < \tfrac{-U_d}{2}) \; u_{a0} = \tfrac{-U_d}{2};$$
$$u_{c0} = \tfrac{R_{off}}{2}i_c; \text{if}(u_{c0} > \tfrac{U_d}{2}) \; u_{c0} = \tfrac{U_d}{2}; \text{if}(u_{c0} < \tfrac{-U_d}{2}) \; u_{c0} = \tfrac{-U_d}{2};$$
$$u_c = -u_{c0} - u_0; \text{if}(K=1) \; u_a = \tfrac{U_d}{2} - u_0; \text{else} \; u_a = -u_{a0} - u_0;\}$$

where $\theta_e = N_p\theta_m$, $\theta_e \in [0°; 360°)$, N_p is number of pole pairs, θ_m is angle of rotor rotation, K is PWM output (Fig. 6). For the next sequence periods:
(b) S1 = S6 = on, S2 = S3 = S4 = S5 = off (HES code: 110)
(c) S3 = S6 = on, S1 = S2 = S4 = S5 = off; (HES code: 010)
(d) S3 = S2 = on, S1 = S4 = S5 = S6 = off; (HES code: 011)
(e) S5 = S2 = on, S1 = S3 = S4 = S6 = off; (HES code: 001)
(f) S5 = S4 = on, S1 = S2 = S3 = S6 = off; (HES code: 101)
the dependencies are analogical.

The second considered control strategy (Fig. 4) for the first sequence period may be described by the following dependencies:

(2)
$$\text{if}(K=1) \; u_d = U_d; \text{else} \; u_d = 0;$$
$$\text{if}(30° < \theta_e \leq 90°)\{u_0 = R_0(i_a + i_b + i_c);$$
$$u_{c0} = \tfrac{R_{off}}{2}i_c; \text{if}(u_{c0} > \tfrac{u_d}{2}) \; u_{c0} = \tfrac{u_d}{2}; \text{if}(u_{c0} < \tfrac{-u_d}{2}) \; u_{c0} = \tfrac{-u_d}{2};$$
$$u_a = \tfrac{u_d}{2} - u_0; \; u_b = \tfrac{-u_d}{2} - u_0; \; u_c = -u_{c0} - u_0;\}$$

As before, for the next sequence periods the dependencies are analogical.

In the case of the third considered control strategy (Fig. 5) one modification was taken into account:

(3)
$$u_d = u_{ref}U_d / U_n$$

The model of BLDC motor with back EMF approximated to the trapezoidal waveform is widely used in computer simulation. The following equations of armature winding voltages and torque were applied in modelling of BLDC motor:

(4)
$$\begin{bmatrix} u_a \\ u_b \\ u_c \end{bmatrix} = R\begin{bmatrix} i_a \\ i_b \\ i_c \end{bmatrix} + \frac{d}{dt}\begin{bmatrix} \psi_a \\ \psi_b \\ \psi_c \end{bmatrix} + \begin{bmatrix} e_a \\ e_b \\ e_c \end{bmatrix}$$

(5)
$$\begin{bmatrix} \psi_a \\ \psi_b \\ \psi_c \end{bmatrix} = \begin{bmatrix} L & M & M \\ M & L & M \\ M & M & L \end{bmatrix}\begin{bmatrix} i_a \\ i_b \\ i_c \end{bmatrix}$$

where $L = L_\sigma + L_\mu$, $M = -L_\mu/3$, L_μ is inductance of main magnetic circuit (magnetization inductance), L_σ is leakage inductance. The following dependency may be used in order to derive the phase currents from the matrix dependency (5):

(6)
$$i_k = (L-M)^{-1}\left(\psi_k - M(L+2M)^{-1}\sum_j \psi_j\right), \quad k,j = a,b,c$$

These currents should be substituted in the equation (4) to reduce the number of unknowns.

Back EMFs:

$$(7) \quad \begin{bmatrix} e_a \\ e_b \\ e_c \end{bmatrix} = N_p \Psi_P \omega_m \begin{bmatrix} f_a(\theta_e) \\ f_b(\theta_e) \\ f_c(\theta_e) \end{bmatrix}$$

where Ψ_P is flux linkage excited by permanent magnets, ω_m is angular velocity of rotor. The following dependency may be adopted in order to approximate the functions f_a, f_b, f_c:

$$(8) \quad \begin{bmatrix} f_a(\theta_e) \\ f_b(\theta_e) \\ f_c(\theta_e) \end{bmatrix} = k_f \begin{bmatrix} \sin(\theta_e) \\ \sin(\theta_e - 120°) \\ \sin(\theta_e - 240°) \end{bmatrix} \quad \cap \quad \begin{matrix} -1 \le f_a(\theta_e) \le +1 \\ -1 \le f_b(\theta_e) \le +1 \\ -1 \le f_c(\theta_e) \le +1 \end{matrix}$$

where $k_f = 2$ for approximation of trapezoidal EMF with wide trapezoid base (120 electrical degrees), $k_f = 1.2$ for approximation of trapezoidal EMF with narrow trapezoid base (about 60 electrical degrees) and $k_f = 1$ for sinusoidal approximation of EMF.

Output (electromagnetic) torque:

$$(9) \quad \tau_e = \omega_m^{-1}(e_a i_a + e_b i_b + e_c i_c)$$

Taking into account Eq. 7:

$$(10) \quad \tau_e = N_p \Psi_P (f_a(\theta_e) i_a + f_b(\theta_e) i_b + f_c(\theta_e) i_c)$$

Results of computer simulation

In the model-simulation investigations the following rated parameters of BLDC motor were taken into account: 4 kW, 400 V, 3000 rpm, 11.5 A, 0.025 kgm^2, $R_s = 0.5$ Ohm, $L_\mu = 7.4$ mH, $L_\sigma = 1.6$ mH, $N_p \omega_m \Psi_P = 212$ V. The carrier frequency of 2 kHz for PWM was adopted.

The selected results of computer simulation are shown in the paper:
1. Results of simulation of BLDC motor energized by PWM-controlled inverter bridge (Fig. 3) are shown in Figs. 7 and 8.
2. Results of computer simulation of BLDC motor energized by the converter system based on PWM-controlled DC/DC converter (Fig. 4) are shown in Figs. 9 and 10.
3. Results of computer simulation of BLDC motor energized by the converter system based on PWM-controlled DC/DC converter and low-pass filter LC (Fig. 5) are shown in Figs. 11 and 12.
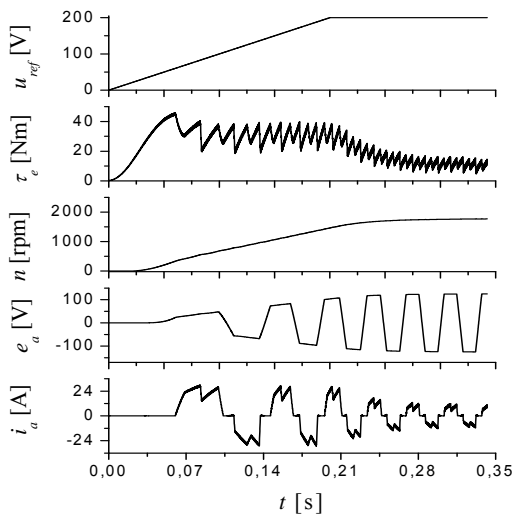

Fig. 7. Reference voltage, output torque, rotational speed, back EMF and phase current during starting the motor
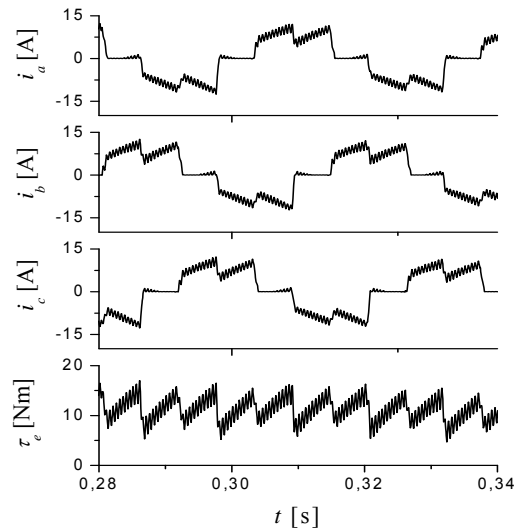

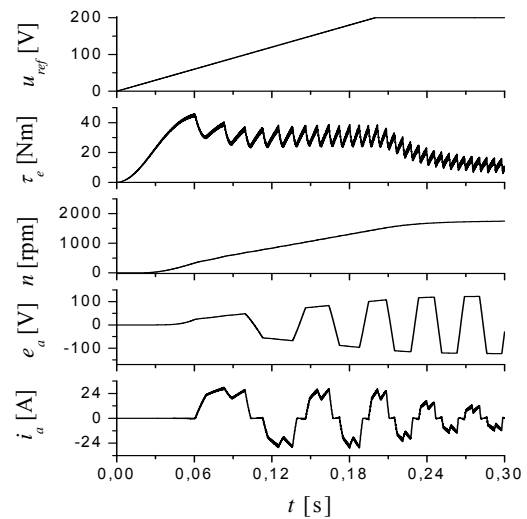Fig. 8. Three-phase current and output torque of BLDC motor under load condition

Fig. 9. Reference voltage, output torque, rotational speed, back EMF and phase current during starting the motor
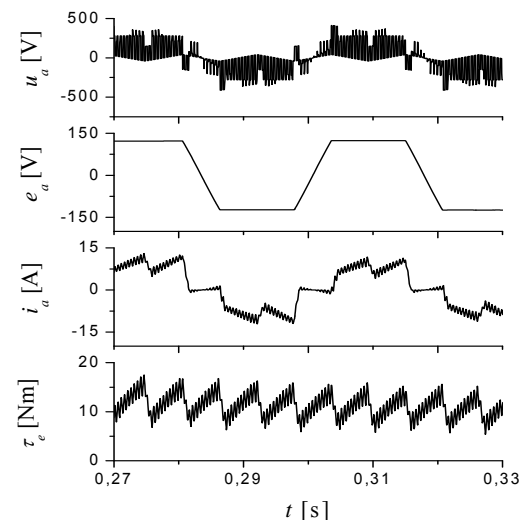

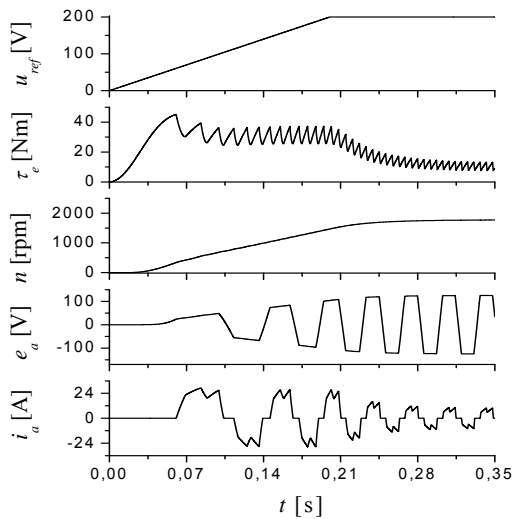Fig. 10. Phase voltage, back EMF, phase current and output torque of BLDC motor under load condition

Fig. 11. Reference voltage, output torque, rotational speed, back EMF and phase current during starting the motor
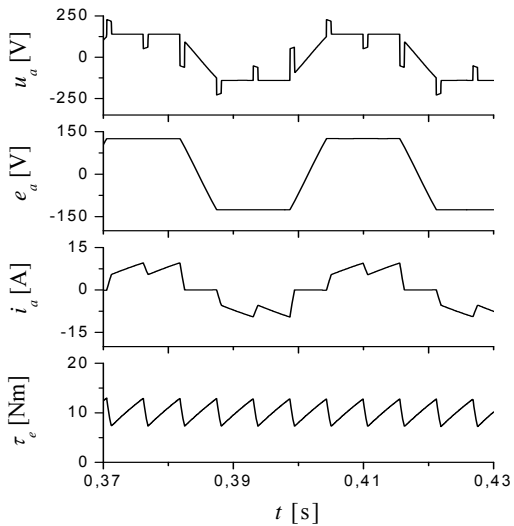

Fig. 12. Phase voltage, back EMF, phase current and output torque of BLDC motor under load condition

Discussion of the results

The results of computer simulation presented in this paper correspond to the experimental results (compare Fig. 8 or 10 and Fig. 13) as well as to the results of other simulation (compare Fig. 12 and Fig. 14).

Various BLDC motor controls, shown in Figs. 3, 4 and 5, give similar dynamic and static behaviour of the motor independently of converter system used to energize the motor. However, there are some differences (compare Figs. 7, 9 and 11 as well as 8, 10 and 12). Time changes of torque and currents of BLDC motor energized by converter system based on PWM-controlled three-phase inverter (Fig. 3) are irregular in contrast to the torque and currents of BLDC motor energized by converter systems based on PWM-controlled DC/DC converter without or with low-pass filter (Figs. 4 and 5). An application of converter system, based on PWM-controlled three-phase inverter or PWM-controlled DC/DC converter without low-pass filter, to energize BLDC motor results in additional high-frequency distortion of currents and torque in contrast to PWM-controlled DC/DC converter with low-pass filter, which, although complicates the structure of BLDC motor control but allows to avoid the occurrence of the abovementioned high-frequency distortion of currents and torque (Figs. 11, 12).
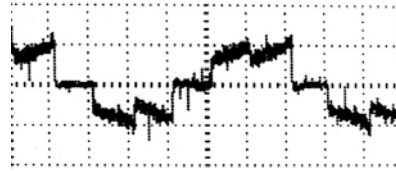

Fig. 13. Measured waveform of BLDC motor phase current using experimental setup [9]
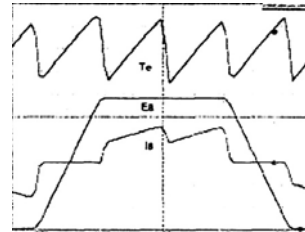

Fig. 14. Output torque, back EMF and phase current using conventional model by IsSpice [10]

Conclusions

The presented mathematical models and results of computer simulation of BLDC motor energized by different types of converter systems give a good base for design activity dealing with BLDC motor control systems. These models and results may be used to verify various control strategies. Computer simulation based on the presented mathematical models of BLDC motor unit can effectively shorten analysis and development cycle of control systems based on BLDC motor as well as evaluate rationality of control algorithm.

Author: *dr hab. inż. Andrzej Popenda prof. nadzw., Politechnika Czę-stochowska, Wydział Elektryczny, Instytut Elektroenergetyki, Al. Armii Krajowej 17, 42-200 Częstochowa, E-mail: apo366@wp.pl.*

REFERENCES
[1] Popenda A., A Control Strategy of a BLDC Motor, *Przegląd Elektrotechniczny*, 89 (2013), nr 12, 188-191
[2] Yedamale P., *Brushless DC (BLDC) Motor Fundamentals*, Microchip Technology Inc., U.S.A., 2003
[3] Rusek A., Chaban A., Lis M., A Mathematical Model of a Synchronous Drive with Protrude Poles, an Analysis Using Variational Methods, *Przegląd Elektrotechniczny*, 89 (2013), nr 4, 106-108
[4] Shchur I., Rusek A., Mandzyuk M., Power Effective Work of PMSM in Electric Vehicles at the Account of Magnetic Saturation and Iron Losses, *Przegląd Elektrotechniczny*, 91 (2015), nr 1, 199-202
[5] Olesiak K., Application of a Fuzzy Logic Controller for a Permanent Magnet Synchronous Machine Drive, *Przegląd Elektrotechniczny*, 92 (2016), nr 12, 113-116
[6] Jakubiec B., Napęd pojazdu elektrycznego z wielofazowym silnikiem synchronicznym z magnesami trwałymi, *Przegląd Elektrotechniczny*, 91 (2015), nr 12, 125-128
[7] Lis M., Algorytm obliczenia wybranych parametrów różniczkowych silnika bezszczotkowego o wzbudzeniu od magnesów trwałych o sterowaniu trapezoidalnym (BLDC), *Przegląd Elektrotechniczny*, 88 (2012), nr 9a, 116-118
[8] Nowak M., Analiza stanów dynamicznych układu napędowego zawierającego silnik BLDC oraz długi element sprężysty, *Przegląd Elektrotechniczny*, 8 (2013), nr 12, 302-305
[9] Giridharan K., Chellamuthu C., Microcontroller Based Model of a Virtual BLDC Motor, *European Journal of Scientific Research*, 75 (2012), No. 2, 179-192
[10] Jeon Y.S., Mok H.S., Choe G.H., Kim D.K., Ryu J.S., A new simulation model of BLDC motor with real back EMF waveform, *Proceedings of the 7th Workshop on Computers in Power Electronics, 2000. COMPEL 2000*, 2000, 217-220
[11] Olesiak K., Badania pomiarowe napędu prądu przemiennego z trójfazowym przemiennikiem częstotliwości, *Logistyka* (2011), nr 6, 3197-3204